

## Enhanced mobility of hydrogenated MO-LPCVD ZnO contacts for high performances thin film silicon solar cells

L. Ding, M. Benkhaira, S. Nicolay, C. Ballif

Ecole Polytechnique Fédérale de Lausanne (EPFL), Institute of Microengineering (IMT),  
Photovoltaics and Thin Film Electronics Laboratory, Rue A.-L. Breguet 2, CH-2000 Neuchâtel

### ABSTRACT

In this contribution, we study the increase in metalorganic-low pressure chemical vapor deposited (MO-LPCVD) ZnO thin films conductivity by hydrogen plasma post-treatment. We show that this improvement is linked to defect passivation at grain boundaries, decreasing the electron traps density and resulting in the almost complete suppression of the electron scattering at grain boundaries. For a 2  $\mu\text{m}$  thick non-intentionally doped ZnO layer, electron mobility reaches after treatment values close to  $60 \text{ cm}^2\text{V}^{-1}\text{s}^{-1}$  (corresponding to an increase of 100%), with a carrier density still as low as  $3 \times 10^{19} \text{ cm}^{-3}$  ( $+1.5 \times 10^{19} \text{ cm}^{-3}$ ). Such layers have an absorbance below 2-3% in the range of 400 to 1100 nm making them among the most transparent and conductive materials reported so far. In addition, we demonstrate that hydrogen plasma post-treated ZnO layers can be used as front electrode for producing highly transparent and conductive electrodes. Eventually, it is shown that hydrogen plasma treatment can also be used on the complete thin film solar cell stack (back contact and silicon device) to improve the cell performances.

### INTRODUCTION

Polycrystalline metalorganic-low pressure chemical vapor deposited (MO-LPCVD) zinc oxide (ZnO) films present, under certain growth conditions [1, 2], V-shaped elongated grains resulting in a self-textured rough surface providing efficient light scattering when used as electrodes in thin film silicon (TF Si) solar cells. The polycrystalline structure of the film implies a strong limitation in electrical conductivity: transport of the charge carriers is indeed mainly restricted by scattering at the potential barrier present at the defective region constitutive of grain boundaries (GB) [3-5]. One way to overcome this limit is to increase the n-type doping, e.g. by addition of group III elements, such as boron. But doping has the inconvenience of increasing the free carrier absorption (FCA), which is detrimental for ZnO transparency. In addition, high doping leads to a higher ionized impurities concentration, also acting as electron scattering centers, which then decreases the intra-grain mobility and hence the conductivity and transparency of the films.

In this work, we apply hydrogen plasma ( $\text{pH}_2$ ) post-treatment onto MO-LPCVD ZnO films to improve film conductivity and to relax the conductivity-transparency trade-off. As a matter of fact, this treatment was reported not only to increase the electron concentration by creating shallow donors, but more particularly to strongly reduce defects density at GB [6-8]. Finally, we show the benefits of  $\text{pH}_2$  post-treatment applied to front and back electrodes of a TF Si solar cell, whereas the benefits could be valid for other types of solar cells or devices using ZnO.

## EXPERIMENTAL DETAILS

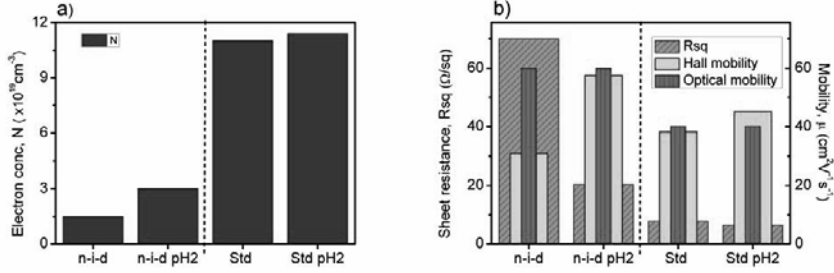
ZnO layers were prepared by MO-LPCVD, on 0.5 mm thick glass substrates, 4x4 cm<sup>2</sup> size. Diethylzinc (DEZ, Zn(C<sub>2</sub>H<sub>5</sub>)<sub>2</sub>) and water vapor were used as precursors for ZnO. Diborane (B<sub>2</sub>H<sub>6</sub>) diluted at 1% in argon was used as the boron dopant source. Further details about the deposition parameters can be found elsewhere [9]. The pH2 treatments were performed in a plasma enhanced chemical vapor deposition (PECVD) reactor, at 200°C, 0.5 mbar, for 20 minutes, with a power density of 12.3 W/cm<sup>2</sup> (200W). P-i-n solar devices were deposited by PECVD also in KAI large-area reactors [10]. A white dielectric polymer was used as back reflector.

The ZnO films were characterized optically using a Perkin Elmer spectrophotometer (lambda 900) equipped with an integrating sphere. An Ecopia Hall effect measurement system (HMS5000) was used to determine the Hall mobility and charge carrier density, in the Van der Pauw configuration, at room temperature. Cell performances were characterized with current-voltage (J-V) measurements using an AM 1.5 Wacom sun simulator with 100 mW/cm<sup>2</sup> light output, in standard conditions. The short-circuit current densities (J<sub>sc</sub>) were evaluated through spectral response measurements.

## DISCUSSIONS

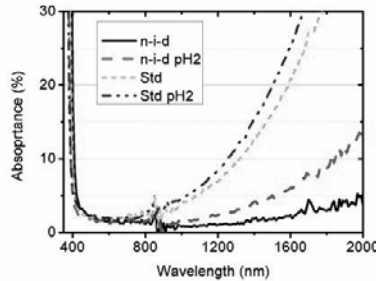
The impact of pH2 post-treatment on the conductivity of ZnO layers was evaluated by treating and characterizing two types of 2 μm thick layers. The first is a non-intentionally doped (n-i-d) film having an initially low Hall electron mobility of 28 cm<sup>2</sup>V<sup>-1</sup>s<sup>-1</sup> and low free electron concentration of 1.3 x 10<sup>19</sup> cm<sup>-3</sup>. The second is a uniformly doped layer, as standardly used as front electrodes for TF Si solar cells (Std), which has a high conductivity thanks to its higher free electron concentration and Hall electron mobility, respectively of 1 x 10<sup>20</sup> cm<sup>-3</sup> and 40 cm<sup>2</sup>V<sup>-1</sup>s<sup>-1</sup>.

Figure 1a) and b) present the electrical properties of the layers as-deposited and after exposure to pH2. It can be seen on Fig. 1a) that N is increased by around + 1.5 10<sup>19</sup> cm<sup>-3</sup> for the two layers. This gain can be ascribed to the insertion of H as shallow donor as well as to release of electrons from passivated traps present at GB [6-8]. In the case of the n-i-d layer, this corresponds to a gain of 100 %, whereas for the Std doped layer, the gain is only ~10%. The electron density gain is accompanied by a strong increase in Hall mobility. As a result of both the improvements in N and μ the n-i-d layer sheet resistance (Rs<sub>q</sub>) is reduced by 70%. It is important to notice here that the Hall mobility trend is reversed after pH2: indeed, in the as-deposited case, the Std layer has a higher mobility than the n-i-d film, as the high density of electrons screens the potential barrier created by trapped electrons at GB [4]. However, after pH2, the Hall mobility of the n-i-d\_pH2 layer is higher than the Std\_pH2 layer, but electron concentration in n-i-d\_pH2 layer is still low. Therefore, this Hall mobility increase is attributed to a reduction of defect states and trapped charges density at GB, resulting in a decrease of the back-to-back Schottky potential barrier. In fact, the mobility of the n-i-d\_pH2 (58.5 cm<sup>2</sup>V<sup>-1</sup>s<sup>-1</sup>) reaches values measured for doped ZnO single crystals with same electron concentration, as reported in [5]. In the same reference paper, comparable Hall mobilities were also reported for magnetron sputtered polycrystalline ZnO films, but having N typically one order of magnitude higher than n-i-d\_pH2.



**Figure 1:** a) Free electron concentration (N) and b) sheet resistance (Rs) and mobility ( $\mu$ ) of n-i-d and std layers as-deposited and after hydrogen plasma post-treatment (pH2)

Figure 1b) also shows the optical mobility as extracted from fitting of the reflectance spectra in the infrared, based on the Drude model [4]. It can be seen that the optical, intra-grain mobility does hardly change in the ZnO layers after pH2 and that the Hall mobility is as high as the optical mobility after the pH2. This is again interpreted as the GB scattering being almost completely eliminated by hydrogen plasma post-treatment and no more limiting the electron transport through the MO-LPCVD grown ZnO films. The n-i-d\_pH2 film containing a low concentration of ionized boron impurities exhibits therefore a higher optical and Hall mobility. This can be explained by the fact that the material surface at GB is “cured” from defects, but that the intra-grain crystallite material is not affected, as its mobility does not increase. Indeed, it is well known that grain boundaries in ZnO can provide fast diffusion path and it is reasonable to think that H ions can easily interact with the surface of the crystallites [11]. In other words: the effect of H ions coming from the plasma would be mainly limited to the GB material.



**Figure 2:** Absorbance spectra of n-i-d and std layers, as-deposited and after pH2.

Regarding the films optical properties, fig.2 shows the absorbance of the layers as-deposited and after pH2. It can be that the spectra are slightly modified for the n-i-d and std layers after pH2. The changes are caused by the slight increase in the free electron concentration. It results both in an increase in transparency due to band-gap widening (Burstein-Moss effect) in the UV and in increased absorption due to free carrier absorption (FCA) in the red-infrared part.

Nevertheless it can be noted that the n-i-d layer exhibits a very high transparency, particularly in the spectral range of Si absorption (370-1100 nm), where the absorption reaches only 2-3%.

### **Hydrogen plasma post-treatment on front and back electrodes**

In this part, 2  $\mu\text{m}$  thick n-i-d ZnO layers, as-deposited and after pH2, were used as front contact substrates for a hydrogenated amorphous silicon (a-Si:H) solar cell of 250 nm i-layer thickness. Co-deposition on a Std ZnO layer was used as reference. Cell performances are presented in Fig. 3a) and b). As discussed in previous section, the pH2 treatment on n-i-d ZnO decreases the  $R_{\text{sq}}$  from  $\sim 80$  to  $20 \Omega/\text{sq}$ . Series resistance losses are therefore decreased in the cell deposited on n-i-d\_pH2, resulting in an improvement in fill factor (FF) (Fig. 3 a)). The cell co-deposited on the Std electrode ( $R_{\text{sq}} \sim 8 \Omega/\text{sq}$ ) still exhibits the highest FF, but generates less photocurrent, as shown in Fig. 3 b). In fact, the Std layer suffers from strong parasitic light absorption (FCA) due to the high doping level. In addition, the high doping produces in the ZnO smaller grains than in the n-i-d, which decreases the light scattering at the ZnO-Si interface [12]. Also, it can be seen that the cell deposited on the n-i-d\_pH2 electrode generates slightly more current in the blue part of the spectrum than on the n-i-d non-treated ZnO, thanks to the widening of its band gap, as discussed in previous section. Actually, this approach should be especially advantageous in the case of tandem amorphous/ microcrystalline  $\mu\text{c-Si:H}$  (micromorph) TF Si solar cells, where the current generation in the bottom  $\mu\text{c-Si:H}$  cell is crucial [13].

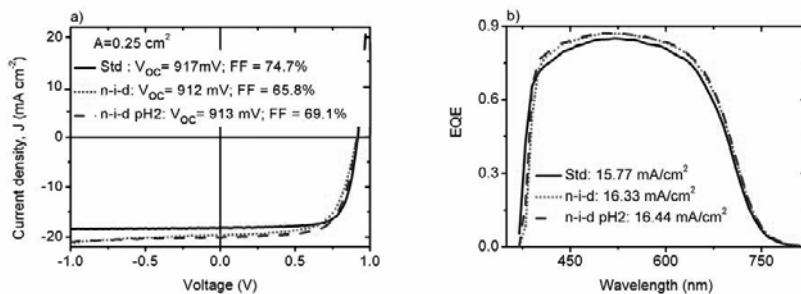


**Figure 3:** Performances of a 250 nm thick amorphous cell deposited on Std, n-i-d or n-i-d pH2 treated front contacts: a) current-voltage and b) spectral response characterizations.

Finally, pH2 post-treatment was applied to a complete micromorph cell, deposited on a pH2 treated n-i-d front contact. The a-Si:H and  $\mu\text{c-Si:H}$  respective i-layer thicknesses were 250 nm and 1.2  $\mu\text{m}$ . On both cells, the back contact was a slightly doped 2.3  $\mu\text{m}$  MO-LPCVD ZnO film. Such a back contact deposited on glass has a  $R_{\text{sq}}$  of  $25 \Omega/\text{sq}$ , that is decreased to  $13 \Omega/\text{sq}$  after pH2. The cell characteristics initially and after pH2 are shown in Fig. 4. It is seen that the micromorph cell gain around 20 mV in  $V_{\text{oc}}$  and almost 1% in FF after pH2. The current densities evaluated though spectral response did not change after pH2. This results in an efficiency increase from 12.6% to 12.85%.

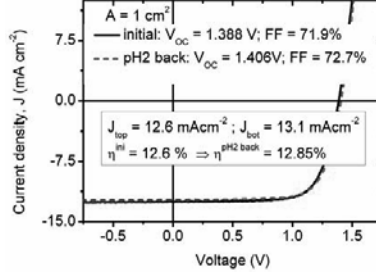


**Figure 4:** Performances (J-V measurement) of a micromorph tandem solar cell initially and after pH2 treatment on the complete cell.

These improvements cannot be attributed to an improvement in ZnO conductivity alone, most probably to a combination of gain in conductivity in the ZnO back contact layer, as well as to an improvement in the Si material quality. Indeed, during the pH2, all the cell sub-layers are exposed to an annealing (under vacuum at 200°C), which is thought to be beneficial to the Si material mainly [14]. Such  $V_{oc}$  increase could however not be reproduced by applying only the annealing step (only + 10mV increase). It is not clear yet what is the exact contribution of the different plasma components (annealing, H ions contact or UV) to the different parts of the stack and this shall be further investigated.

## CONCLUSIONS

It was shown that the most significant effect of pH2 treatment on MO-LPCVD ZnO films is the passivation of defects at grain boundaries, which was manifested by Hall mobility value as high as optical mobility. This means that the electron transport in the layers was no more limited by GB scattering, but by ionized impurities scattering, even for electron concentration  $< 4 \times 10^{19} \text{ cm}^{-3}$ . In addition to the effect on ZnO layers, a direct positive impact on cell performances (FF,  $V_{oc}$ ) could be observed, when pH2 was applied to front and back ZnO electrodes of TF Si, a-Si:H or micromorph cells.

## ACKNOWLEDGMENTS

The authors would like to thank Mathieu Charrière and Grégory Bugnon for the developments of the amorphous and microcrystalline silicon solar cells, respectively. We would also like to thank Dr. Jérôme Steinhauser for fruitful discussions.

This work was supported by the Swiss Federal Office of Energy (OFEN) (grant No. 101191) and by the EU FP7 “N2p” project (Grant No CP-IP 214134-2 N2P).

## REFERENCES

1. S. Nicolay, S. Fay<sup>®</sup> and C. Ballif, *Cryst. Growth Des.* **9**, (11), pp 4957–4962 (2009)
2. Wenas, Wilson W., Yamada, Akira, Takahashi, Kiyoshi, Yoshino, Masahiro, Konagai, Makoto, *J. Appl. Phys.* **70**, 7119-7123 (1991)
3. J. Y. W. Seto, *J. Appl. Phys.* **46**, 5247 (1975)
4. J. Steinhauser, S. Fay, N. Oliveira, E. Vallat-Sauvain, C. Ballif, *Appl. Phys. Lett.* **90**, 142107 (2007)
5. K. Ellmer, *J. Phys. D: Appl. Phys.* **34**, 3097-3108 (2001)
6. C. G. Van de Walle, *Phys. Rev. Lett.* **85**, 86 (2000)
7. Cai, P. F.; You, J. B.; Zhang, X. W.; Dong, J. J.; Yang, X. L.; Yin, Z. G.; Chen, N. F.; J. *Appl. Phys.* **105**, 083713 (2009)
8. J. J. Dong, X. W. Zhang, J. B. You, P. F. Cai, Z. G. Yin, Q. An, X. B. Ma, P. Jin, Z. G. Wang and Paul K. Chu, *Appl. Mater. Interface* **2**, 6, 1780-1784 (2010)
9. L. Ding, M. Boccard, G. Bugnon, M. Benkhaira, S. Nicolay, M. Despeisse, F. Meillaud and C. Ballif, *Sol. Energy Mater. Sol. Cells* **98**, pp. 331-336 (2012)
10. M. Despeisse, C. Battaglia, M. Boccard, G. Bugnon, M. Charrière, P. Cuony, S. Hänni, L. Löfgren, F. Meillaud, G. Parascandolo, T. Söderström, and C. Ballif, *Phys. Status Solidi A*, 1-6, (2011)
11. W. Beyer, F. Hamelmann, D. Knipp, D. Lennartz, P. Prunici, A. Raykov, H. Stiebig, *Proc. 25th European Photovoltaic Solar Energy Conference* (2010)
12. S. Fay, L. Feitknecht, R. Schluchter, U. Kroll, E. Vallat-Sauvain, and A. Shah, *Sol. Energy Mater. Sol. Cells* **90**, 2960 (2006)
13. M. Boccard, P. Cuony, C. Battaglia, M. Despeisse, C. Ballif, *Phys. Status Solidi RRL* **4** (11), 326–328 (2010)
14. S Veprek, Z Iqbal, R O Kuhne, P Capezzuto, F -A Sarott and J K Gimzewski, *J. Phys. C: Solid State Phys.* **16**, 6241-6262 (1983)